Appendix SI for "Genetic manipulation of structural color in bacterial colonies" by Johansen et al., 2018

Please note that references to Figure 1-5 are to the main manuscript and Movie S1 to an external video file. The extended Materials and Methods are presented first, followed by Supporting Information (SI), then SI tables, and then SI figures.

Materials and Methods

Isolation and identification. Strain IR1 was isolated on ASW agar (see Table S1) on the basis of simultaneous resistance to the antibiotics colistin (MIC 10 μg/ml) and cefotaxime (MIC 50 μg/ml) during a screening of estuarine sediment samples from the Neckarhaven region of Rotterdam harbour. Strain IR1 is a yellow-pigmented Gram-negative bacterium culturable on ASW agar under aerobic conditions from 2 to 30 °C. On ASWB plates, containing nigrosine as a contrasting agent, IR1 formed intensely structurally coloured green colonies with red/orange edges as seen in Fig. S11.

Culture conditions. All Flavobacterial strains were grown at 20 °C under aerobic conditions unless stated otherwise. Culture media are summarised in Table S1. Agarose was used as a gelling agent in most cases, solidified with the lids of the Petri dish on a flat surface, to provide an optically flat surface for imaging. F52 and F52 *gld*J were obtained from the Cytryn laboratory and grown on ASWB agar with the addition of 20 μg/ml of tetracycline in the latter case. Viable counts were made on ASWB agar unless noted otherwise. Structurally coloured colonies of IR1 on ASWB agar appeared after inoculation for 8 to 30 h at 20 °C, see Fig. S8. A standard medium with 1% (w/v) KCl or artificial sea salts was used. We observed that salinity from 0.5 to 1.5% (w/v) supported optimal growth for bright colouration, higher and lower salinity mediums allowed growth but less intense colouration. These optimal conditions match the salinity of the location from which the bacterium was isolated. The colony edges showed tiered layers of cells that glided over each other and over the agar (Fig. S8A-B).

Transposon mutagenesis. A transposon system was used to generate libraries from IR1. A screening of an IR1 library of over 20,000 colonies on ASWBC medium generated dull mutants, i.e. colonies with diminished structural colour, at a frequency of 1/250; black mutant, i.e. knockouts with no structural colour, at 1/1,200; and mutants with intense but colour-shifted iridescence at 1/1700. Screening on ASWBC plates, with κ-carrageenan as the sole gelling agent, increased the frequency of colour-shifted mutants to 1/500 with 1/2100 black mutants and 1/300 dull. Mutants with different structurally coloured appearances are presented in Fig. 1, and a complete list of mutants is presented in Table S3.

Genome sequencing and assembly. The isolated genome of IR1 is sequenced by Illumina Hi-seq paired-end technology, which resulted in 5220986 paired end reads (forward reads and reverse reads) with an average GC content of 36% and read length of 251 base pairs. Subsequent processing and assembling was performed on a Galaxy server running Trim Galore (3.6.) followed by contig. assembly in SPAdes 3.6.2 (1) with gene prediction using Prodigal 2.6 (2). Genome browsing was performed with Artemis (3) and synteny analysis with Geneious R9.1 (4) www.geneious.com.

Identification of strain IR1. A 1368 bp fragment of the 16S from the assembled IR1 genome was used to identify related 16S rRNA sequences from the RDP, Greengenes and Genbank databases. Phylogenetic trees were constructed using SeaView version 4.6.1 (5).

Killing, fixation and scanning electron microscopy of IR1. The colonies were killed by adding 50 mg of iodine crystals in the lid of the petri dish used to culture the bacteria, then sealing with parafilm and incubating for 6 to 12 h. To fix the bacteria, plates with iodine-killed cells were treated in one of two ways: (A) flooded with fixative (phosphate buffered saline with 0.5% (v/v) glutaraldehyde). In this scenario, the colonies could be floated off the agarose surface and captured on SEM grids (EMS Supplies, NL). (B) Poly-L-lysine coated coverslips (12 mm diameter, BDH, NL) were placed on top of the colonies, then the fixative gently pipetted at the edge of the cover slip so it was diffused under the glass. After 2 h the coverslip was picked up with tweezers, with the entire colony adhering to the coverslip. For both routes, subsequent treatments with osmium tetroxide, acetone dehydration and critical point drying were as previously described (6). In the case of method (B), the colonies were inverted, but presented with the right side up for imaging.

Determining cell shapes from SEM images Bacteria cell length and diameter were determined from several SEM images by manual measurements using ImageJ (7) www.imagej.net. Roughly 150 measurements were taken for each parameter. The data can be recovered from doi.org/10.17863/CAM.16794. Due to the M17 cells extending beyond image frames on most images, a lower count was used here probably excluding the longest ones and biasing the result. The margin of error (ME) was with 95% confidence ($z = 1.96$) determined to be less than 5% of the average using the formula $ME = z\sigma/\sqrt{N}$ for all cases except the length of M17 where not enough data could be acquired due to bacteria lengths exceeding SEM image size.

Autocorrelation. Autocorrelation was obtained by 2D convoluting the image with a version of the image with axis directions inverted. The result was then normalised so that the maximum correlation (when the two images are exactly overlapping) is 1. Since the convolution was implemented using Fast Fourier Transforms (FFT), sections of 512×512 pixels were analysed. The extracted lines shown in the text were found as the direction with most signal and followed the direction of bacteria ordering. Those lines were furthermore Fourier transformed (this time using 1D FFT) in order to assess correlation frequency - and by that, the repetition frequency of the bacteria. The inverse of this frequency corresponds to the period of the cell organisation. The scripts used to generate the plots are available from doi.org/10.17863/CAM.16794.

Angle-resolved scattering measurements (goniometry). Angle-resolved spectral scattering measurements were carried out using a custom-made goniometer (8). The bacteria were illuminated by a xenon lamp (HPX2000, Ocean Optics) coupled through a fibre to a reflective collimator (RC08SMA-F01) in order to produce a collimated beam with a spot size of roughly 8 mm. Scattered light was detected by the same type of reflective collimator connected through a fibre to a spectrometer (AvaSpec-HS2048, Avantes). The collimator was mounted on a motorised rotation stage. The bacteria samples were mounted on another motorised rotation stage with a coinciding rotation centre. Incident light angle was then changed by rotating the sample, and angular scattering recorded by rotating the detector. The bacteria samples were prepared on a thick agar substrate with added nigrosin in order to minimise unwanted reflection from the substrate.

Measurements were either taken in a specular reflection configuration, where specular reflection was recorded for different incident angles; or scattering configuration, where the incident angle was kept fixed and scattered light recorded by moving the detector. Integration time was automatically determined by the scanning software, but usually around 50-300 ms for specular reflection and 1-3 s for scattered light recordings. The angular resolution was kept at 0.5°, meaning that the sample would normally be mounted for 1-2 h. A specular recording of a white diffuser at 5° incidence was used for normalisation.

Analysis of scattering response. Goniometer measurements of light scattering from the different strains show reflection behaviour caused by their structural organisation. This appears as diffraction spots in the scattering measurements. Due to the regular ordering of the bacteria, the angles at which diffraction spots can occur are given by the grating equation,

$$\theta_m = \arcsin\left(\frac{m\lambda}{d} - \sin\theta_i\right), \qquad [1]$$

where m is the so-called diffraction order and can take up any integer value, λ is the wavelength, d is the period and θ_i is the

illumination angle. This equation can be used to determine the period (d) of the bacteria organisation, and deviation from the predicted diffractions spots can quantitatively inform about the degree of disorder compared to an ideal periodic structure.

Screening for compounds affecting iridescent growth. ASWBC and ASWBLow plates were spread with IR1 so that iridescence would form after 12 to 24 h with iridescence being lost after 4 to 6 days. Test compounds and materials were spotted onto the plates at 0 h, incubated up to a week to test enhancement of the formation of iridescence and maintenance beyond the normal time span. An additional screen was made by repeating this procedure by spotting on plates after 6 days when structural colour had faded. When compounds were identified, these were retested at defined concentrations within agar plates.

Screening for natural surfaces supporting iridescence. Structural colour of IR1 was screened for on materials collected from Rotterdam Harbour, including macroalgae and biofilm covered rocks from Neckarhaven and Europort regions (NL). Additionally, red, brown and green macroalgae were purchased fresh from Just Seaweed, UK including *Chondrus crispus* (Irish moss), *Fucus vesiculosus* (marine bladder wrack), *Saccharina japonica, Ulva lactuca, Ulva intestinalis, Pelvetia canaliculata, Ascophyllum nodosum*. Other macroalgae were obtained dried from health food outlets, including 'nori' grades of Pyropia, i.e. the red algae *P. tenera* and *P. yezoensis*, as well the brown alga *Hizikia fusiforme*, *Eisenia bicyclis* and *Undaria pinnatifida* (wakame). The hydrated algae were partially embedding the sample in agar with 1% (w/v) KCl with a portion of the material exposed which was inoculated with strain IR1. Incubation was for up to 4 weeks under humidified conditions.

Transposon mutagenesis and mapping. The HiMar transposon system was delivered into IR1 as previously described for other *Flavobacteria* (9), except that the IR1 for conjugation were scraped directly from an ASW plate. Screening was on ASWBC plates unless stated otherwise, except that the concentration of agarose was increased to 2% (w/v) to increase the separation between potentially motile colonies. Mutants with altered iridescence properties were recovered after 4 to 6 days. Genomic DNA was prepared from potential mutants using a DNeasy Kit (Qiagen, NL). Transposon insertions were mapped by excision of the transposon (plus flanking sequences) from the IR1 genome. Plasmid recovery was into *E. coli* followed by plasmid purification (GenElute Plasmid Miniprep Kit, Sigma, NL) followed by DNA sequencing of the recovered insert (9). Transposon insertion sites were mapped on the IR1 genome using BlastN searches. Low coverage genome sequencing (GATC Biotech, Germany) was used to check that transposon insertion points were mapped correctly and that there was only a single transposon insertion in a genome. The Geneious bioinformatics package (version R9, Biomatters, US) was used to investigate the predicted function of genes and predicted polypeptides and to perform synteny analysis in comparison with other Flavobacterial genomes.

Observations of motility. Colony expansions rates (being primarily limited by motility rather than growth rate) were calculated from the advancement of colony edges (at least 5 measurements averaged) from images taken over 30 min to 2 h using an Olympus BX-41 microscope, with the measurement of distances using ImageJ 1.45S (7) www.imagej.net.

Screening for the effects of volatiles. Where the objective was to look at the motility and iridescence of IR1, the ASWB agar plate was inoculated in the centre with 5 μl of IR1 containing 10^7 viable cells resuspended in phosphate buffered saline. To investigate the effect of any volatiles triggered by growth of IR1 or from algae, the setup was changed such that two agar plates were taped together to create a 6 mm air gap between the two agar surfaces which were directly facing each other. The upper plate was designated the recipient plate and was inoculated as described above, the lower plate was the donor plate and contained ASWB agar, supplemented with 2% (w/v) κ-carrageenan or fucoidan as appropriate. Alternatively, the donor plate contained 10 g of a macroalgae embedded in 10 ml of 1% (w/v) KCl gelled with agarose. The donor plate was spread with 10^9 cells of IR1 or left without inoculation as a control. After set up, plates were sealed with parafilm and incubated at 20 °C.

Supporting Information

Additional information on bacteria isolation and mutation. The different culture media used is listed in Table S1. The wild type strain IR1 was screened for colouration and duration on a series of different modifications to the ASWB base with the results being presented in Table S2. A phylogenetic tree including IR1 and previoulsly known iridescent strains is displayed in Fig. S1. An overview of mutants of IR1 derived from transposon mutagenesis is available in Table S3. Furthermore, a genetic and phenotypic analysis of M5 and M16 is shown in Fig. S2.

Angle-resolved scattering from IR1 wild type and mutants. Each mutatant shows a different photonic response based on their different organisational capabilities and cell dimensions. Fig. S3 provides goniometer data for different strains recorded at three different light incident angles as well as a specular scan where incident angle equals recording angle ($\theta_{in} = \theta_{out}$). The data show how the different mutations and wild type assemble with different periodicities and how both strong and weak diffraction spots can be observed, as well as none at all. Lines have been overliad according to the grating equation in Eq. 1 in order to predict the period of the structure. For each strain, the three scattered plots are plotted on the same colour scale. The specular reflection is on a separate colour scale. Data for a blank substrate is given as well to give an idea of how this influence the recordings at lower wavelengths.

Independence of φ-rotation. The data in Fig. S4 show goniometer recording of the wild type IR1 for different φ rotations (see Fig. 3D) and incident angles. From this we concluded that the in-plane orientation of the bacterial colonies does not affect our measurements. The fading of signal and slight shift in diffraction spot location is ascribed to the drying of the sample from continous illumination of the light source required to take the repetitive measurements at several orientations. All plots are to the same scale, and the large yellow areas are saturated values due to the intensity of the specular reflection.

Peak extraction. To further increase understanding of the relation between photonic response and structural arrangement, the angle-resolved peak intensities around the lower diffraction spots were extracted and plotted for comparison, see Fig. S5A. It is seen that WT have a more narrow peak than M16, whereas the distance between peak and background is largest for M16. The narrow WT peak could be caused by the low variation in diameter (Fig. S6A) that causes low variation in the cell-to-cell distance on the short range and therefore a more well-defined grating spot. The lower background for M16 could be caused by their ability to keep order over long ranges as described in the text and further supported by Fig. S7. A better kept ordering would mean less scattering in directions in between grating spots. M17 have a barely distinguishable peak, but from the analysis in Fig. S3 it is confirmed that the increase in intensity is indeed due to structural organisation.

Bacterium dimensions from SEM. We assessed bacterium length and diameter from a range of SEM images in order to correlate shape and variation to the observed optical response as described in the main text. The statistics is presented in Figure S6.

Autocorrelation analysis. The SEM images in Fig. 2A-D have been analysed using image autocorrelation. This information tells about to what degree the orientation and position of a cell can be predicted given its distance from a known cell (corresponding to high correlation). Fig. S7A-D show autocorrelations for the wild type and three mutants, with Fig. S7E-H showing extraced lines from the plot where the correlation is largest. M16 have an ordering that extends much further than any of the other strains, which corresponds well with the optical analysis and the conclusions in the main text and Fig. S5. The autocorrelation of the WT is less pronounced but still reveals a regular periodic arrangement on a shorter scale. The organisation of M5 is only keptover small distances, and no detecable correlation is possible for M17. The Fourier transforms of the line plots (Fig. S7I-L) further elucidate the difference, with M16 having a well-defined peak and no observable peak for M17. From the Fourier transform peaks, the periodicity of the different cell organisations on the SEM images can also be calculated as 376 nm, 526 nm, 365 nm, – respectively.

Motility and iridescence of IR1 and F52. The relation between gliding motility and structural colour is investigated in Fig. S8, where both colony growth and colouration is assessed for WT, M17 and the *Flavobacterium* F52.

Hydrated, fixed colonies of IR1. The bacterial colonies can be fixed while still retaining structural colouration, see Methods for protocols. This was used for microscopy using SEM. The appearance of fixed samples is shown in Fig. S10.

Further details on colour formation. Fig. S11 shows the structural colouration for a typical IR1 sample. The Movie S1 shows the rapid formation of structural colour after a coloured area of bacteria was scraped away.

1. Bankevich A, et al. (2012) Spades: A new genome assembly algorithm and its applications to single-cell sequencing. *Journal of Computational Biology* 19(5):455–77.
2. Hyatt D, et al. (2010) Prodigal: prokaryotic gene recognition and translation initiation site identification. *BMC Bioinformatics* 11(119).
3. Rutherford K, et al. (2000) Artemis: sequence visualization and annotation. *Bioinformatics* 16(10):944–5.
4. Kearse M, et al. (2012) Geneious basic: an integrated and extendable desktop software platform for the organization and analysis of sequence data. *Bioinformatics* 28(12):1647–49.
5. Gouy M, Guindon S, Gascuel O (2010) Seaview version 4: A multiplatform graphical user interface for sequence alignment and phylogenetic tree building. *Molecular Biology and Evolution* 27(2):221–4.
6. Ingham CJ, et al. (2007) The micro-petri dish, a million-well growth chip for the culture and high-throughput screening of microorganisms. *Proceedings of the National Academy of Sciences* 104(46):18217–22.
7. Schneider CA, Rasband WS, Eliceiri KW (2012) Nih image to imagej: 25 years of image analysis. *Nature Methods* 9:671–5.
8. Vignolini S, Moyroud E, Glover BJ, Steiner U (2013) Analysing photonic structures in plants. *Journal of the Royal Society Interface* 10(20130394).
9. Braun TF, Khubbar MK, Saffarini DA, McBride MJ (2005) *Flavobacterium johnsoniae* gliding motility genes identified by *mariner* mutagenesis. *Journal of Bacteriology* 187(20):6943–52.

Name	Components (per litre)
ASWB	5 g KCl, 5 g peptone (Sigma, NL:70173), 1 g yeast extract (Sigma, NL: Y1625), 100 mg nigrosine (Sigma NL:N4754), 15 g Bactoagar (BD) or agarose (Eurogentec). Agar was used for routine culture, agarose for imaging applications.
ASWBC[1]	As ASWB with the addition of 5 g κ-carrageenan (Sigma, NL: 22048).
ASWBF	As ASWB with the addition of 2.5 g fucoidan (Absonutrix, US).
ASWBS	As ASWB with the addition of 5 g soluble starch (Sigma, NL: S9765)
ASWBLow[2]	As ASWB but without the peptone.
ASWLow	As ASWBLow without nigrosine.
ASWBVLow[3]	As ASWBLow but with only 50 mg yeast extract.

[1] Standard medium for comparing structural colour in WT and mutants.
[2] Standard low nutrient medium.
[3] Standard near-starvation medium.

Table S1. Culture media for IR1. All culture media were adjusted to pH7.4 and autoclaved.

Modification to ASWB base[1]	Colouration score[2]	Duration[3] (d)
None	+ green	1-6
No nigrosine	+ green[4]	1-6
No KCl	+/- green	3-6
2% KCl (w/v)	+/- green	3-6
3% KCl (w/v)	-	
1% sea salts (w/v), no KCl	+ green	1-6
2% sea salts (w/v), no KCl	+ green	1-6
3% sea salts (w/v), no KCl	+ green	1-6
0.5% κ-carageenan (w/v)[5]	++ green	1-6
2% ι-carrageenan	+ green	1-6
0.25% fucoidan (w/v)	++ green/blue	1-8
2% fucoidan (w/v)[6]	+ blue	1-6
2% soluble starch (w/v)[7]	++ green/blue/purple	1-6
0.1 mm ferric ammonium citrate	++ green	1-3
No peptone[8]	+ green	2-8
No peptone, only 200 mg/l yeast[9]	+ green	2-8
0.5 mm p-nitrophenyl glycerol[10]	+/- green/blue	4-8
2% agarose (w/v)[11]	+ green	1-6
3% agarose (w/v)[12]	+/- green	1-6
4 °C	+/- green/blue/purple	5-20
28 °C	+ green	1-4

[1] See Table S1. Incubation was at 20 °C unless stated otherwise.
[2] Scored for intensity and dominant colour(s). +/- indicates residual but detectable iridescence as also found in a dull mutant and scored as – is the equivalent of an iridescent KO or dark mutant.
[3] Number of days with observed structural colour.
[4] Colour harder to visualise without dark background.
[5] ASWBC medium – see Table S1.
[6] ASWBF medium – see Table S1.
[7] ASWBS medium – see Table S1.
[8] ASWB Low medium – see Table S1.
[9] ASWBS VLow medium – see Table S1. Motility enhanced from 0.7 mm/day on ASWBC to > 1 cm/day.
[10] Motility delayed.
[11] Limited motility, 4 mm/day.
[12] No detectable motility.

Table S2. Overview of growth conditions regulating structural colouration.

Mutant (exemplar)	Other mutants with transposon insertion within same gene as exemplar	Gene product and/or pathway	Phenotype on ASWBC agar
*gmp*1::HiMar (M1)		Guanosine monophosphate synthetase (GMPS)	Disorganised, dull iridescence, curved elongated cells
*spo*T5::HiMar (M5)		SpoT / stringent response	Motile, very disorganised
9::HiMar (M9)		Acriflavine resistance gene	
10::HiMar (M10)		NAD-malic enzyme / citric acid cycle	Disorganised, dull colour
*spr*F12::HiMar (M12)		SprF / Gliding and adhesion	Disorganised, not motile, dull colour
*hpy*A16::HiMar (M16)	*hpy*A8::HiMar (M8), *hpy*A43::HiMar (M43), *hpy*A54::HiMar (M54), *hpy*A70::HiMar (M70), *hpy*A79::HiMar (M79), *hpy*A84::HiMar (M84), *hpy*A79::HiMar (M79), *hpy*A103::HiMar (M103), *hpy*A108::HiMar (M108), *hpy*A115::HiMar (M115), *hpy*A130::HiMar (M130)	Hypothetical A (unknown role in cell organisation)	Highly organised, short cells packed tightly, red shifted colour.
*gldi*A17::HiMar (M17)	*gldi*A6::HiMar (M6)	GldA / gliding but not found in *F. johnsoniae*	Disorganised, poorly motile
19::HiMar (M19)		Homogentisate dioxygenase / tyrosine degradation	Slightly disorganised, brown pigment, dies rapidly
*sul*P22::HiMar (M22)		SulP transporter	Highly organised but blue shift
*spr*B23::HiMar (M23)	*spr*B140::HiMar (M140), *spr*B147::HiMar (M147), *sprB*150::HiMar (M150)	SprB / gliding and adhesion	Disorganised, poorly motile, dull green
*GH3*40::HiMar (M40)	*GH3*45::HiMar (M45)	GH3 / auxin response element	Looks WT but becomes dull faster than WT (2 days)
41::HiMar (M41)		Heme synthesis	Intense green like WT with red colour after 1-2 days.
47::HiMar (M47)	61::HiMar (M61), 73::HiMar (M73)	Non-ribosomal peptide synthesis	Dull green/blue
49::HiMar (M49)	64::HiMar (M64)	tRNA methyltransferase	Poor growth, not iridescent, non-motile
*mal*Y51::HiMar (M51)		Maltose transporter	Gains structural colour faster than WT
*hyp*N52::HiMar (M52)		Hypothetical	Gains structural colour faster than WT
*hk*65::HiMar (M65)		Histidine kinase	Bright green with blue in centre
74::HiMar (M74)		Transcriptional regulator	Intense blue, rapidly spreading colony
76::HiMar (M76)	77::HiMar (M77), 142::HiMar (M142)	UDP-glucose dehydrogenase	Dull green
86::HiMar (M86)	88::HiMar (M88)	Putative endoxylanase	Dull blue
116::HiMar (M116)		Hypothetical	Red shifted
*wsx*141::HiMar		MATE family protein	Dull green structural colouration, non-motile
148::HiMar (M148)		Type I restriction-modification system	Dull structural colour

Table S3. Overview of mutants derived from transposon mutagenesis.

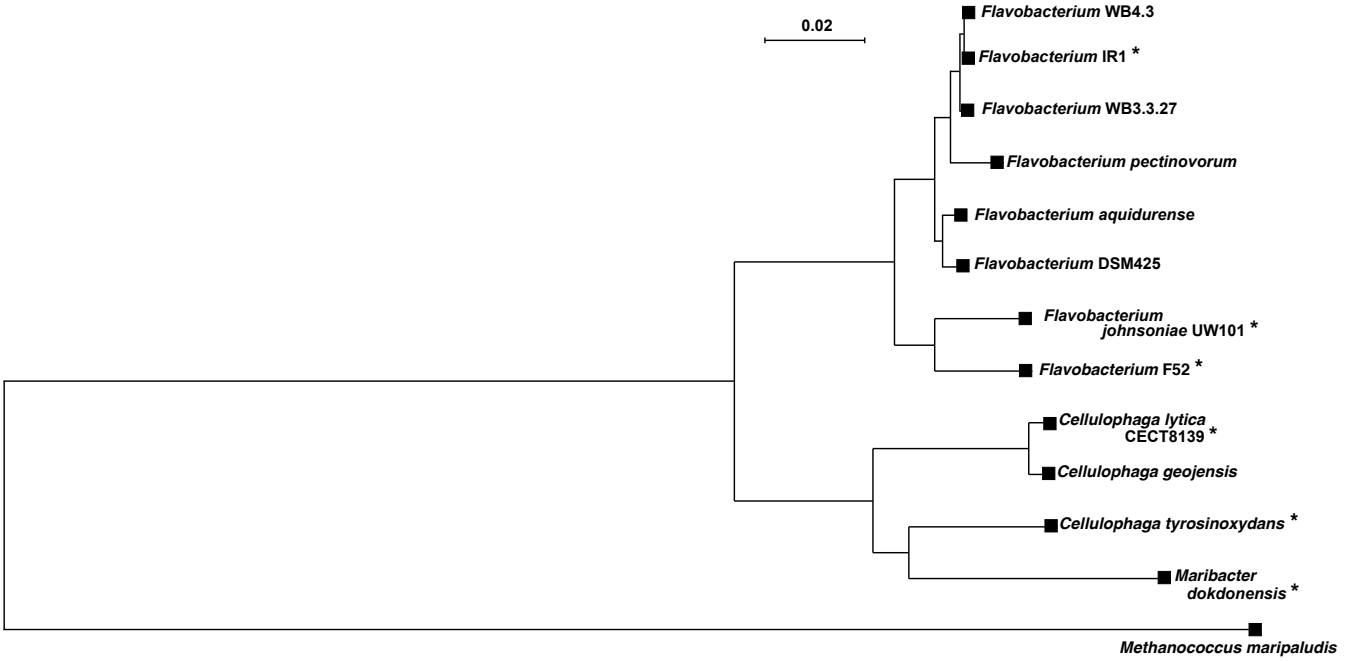

Fig. S1. Phylogenetic tree based on 1368-bp region of the 16S rRNA sequences showing strain IR1 relative to flavobacteria and members of the Cytophaga-Flavobacterium-Bacteroides phylum. Neighbour joining tree was constructed using SeaView version 4.6.1 software with Jukes and Cantor substitutional evolution model and 1000 bootstrap resampling analysis. A star (*) indicates known iridescent strains. The scale bar indicates nucleotide substitutions per site.

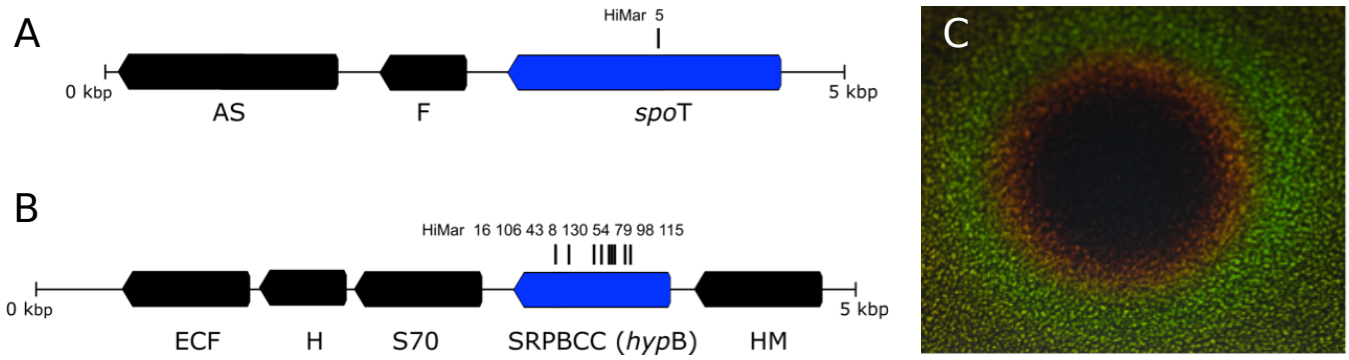

Fig. S2. Genetic and phenotypic analysis of M5 and M16. A) Mapping transposon insertion from mutant 5: AS, gene encoding Adenyl succinate synthetase; F, gene encoding Fur family transcriptional regulator; *spo*T, ppGpp synthetase/hydrolase. B) Transposon insertion for mutant 16. ECF gene encoding extracytoplasmic sigma factor, H hypothetical, S70 sigma70, HM=hypothetical membrane protein. C) Photograph of WT strain cultured on ASWBLow agar with $2\ \mathrm{mg}$ DL-serine hydroxamate in the centre, showing suppression of structural colour ($18\ \mathrm{mm}$ diameter dark area) giving the same phenotype as M5 with growth, motility but disorganised cells without structural colour.

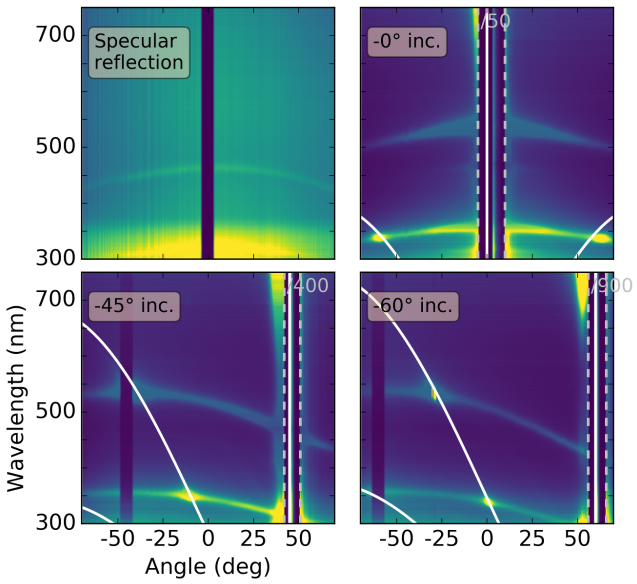

WT The grating period for the overliad lines was set to $400\ \mathrm{nm}$.

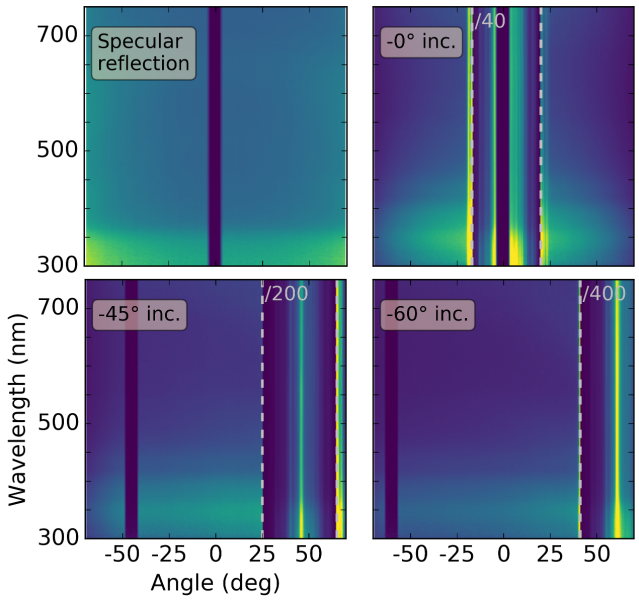

M5 Apart from a broadened specular reflection, no scattering due to structural organisation is oberseved.The diffuse scattering at low wavelengths is most likely caused by the substrate (see measurement on blank substrate).

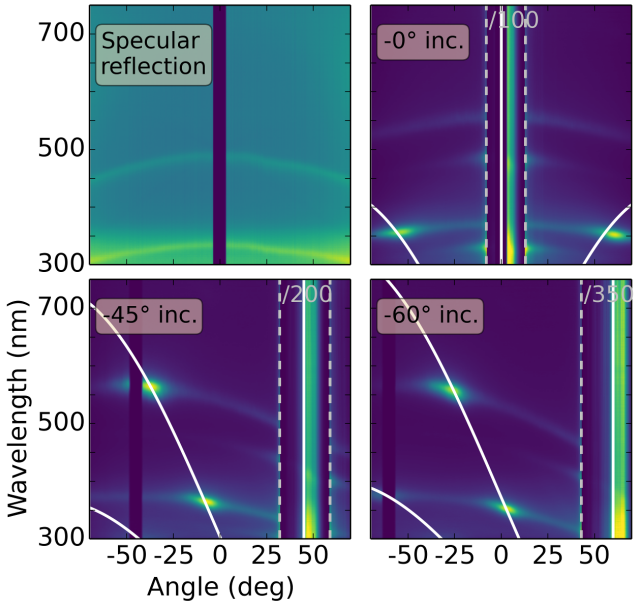

M16 The grating period for the overlaid lines was set to $430\ \mathrm{nm}$.

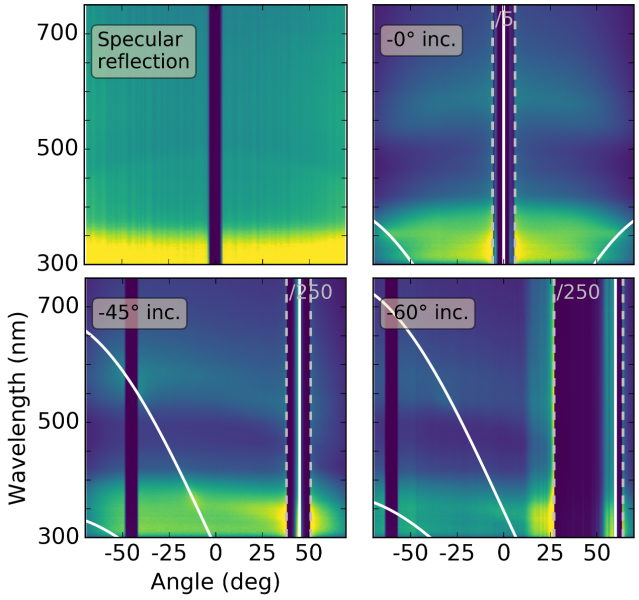

M17 The grating period for the overlaid lines was set to $400\ \mathrm{nm}$. Notice how the weak diffraction spots lie on the lines following the grating equation for different input angles. This confirms that these weak spots indeed do originate from the (weak) periodic arrangement of the colony.

Fig. S3. Scattering goniometry and specular reflectance data for different mutants. (continues on next page)

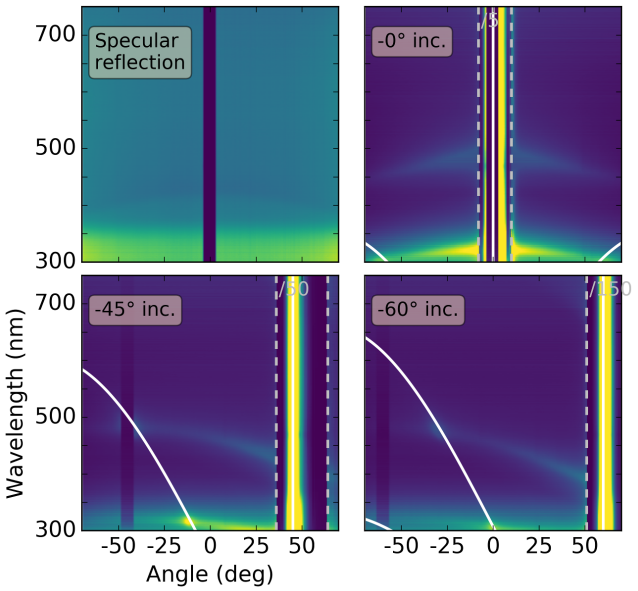

M80 The grating period for the overlaid lines was set to $355\ \mathrm{nm}$.

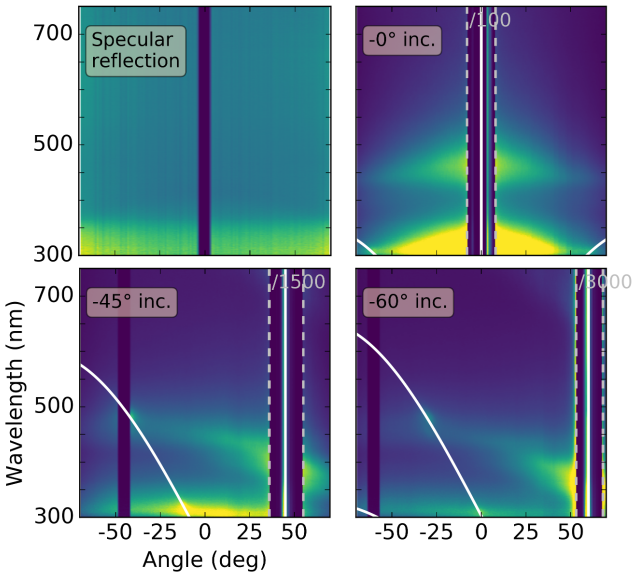

M83 Diffraction spots are weaker than most other ordered strains. Periodicity is $350\ \mathrm{nm}$.

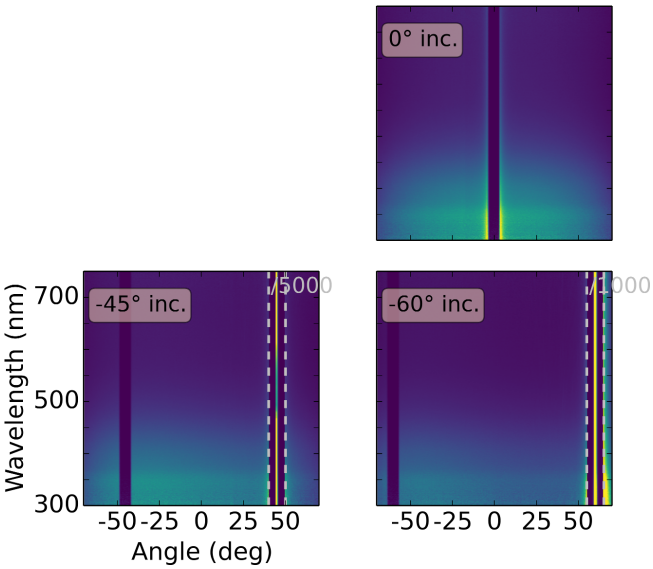

Blank substrate Typical substrate used for measurements, but without bacteria.

Fig. S3. (cont'd) Scattering goniometry and specular reflectance data for different mutants.

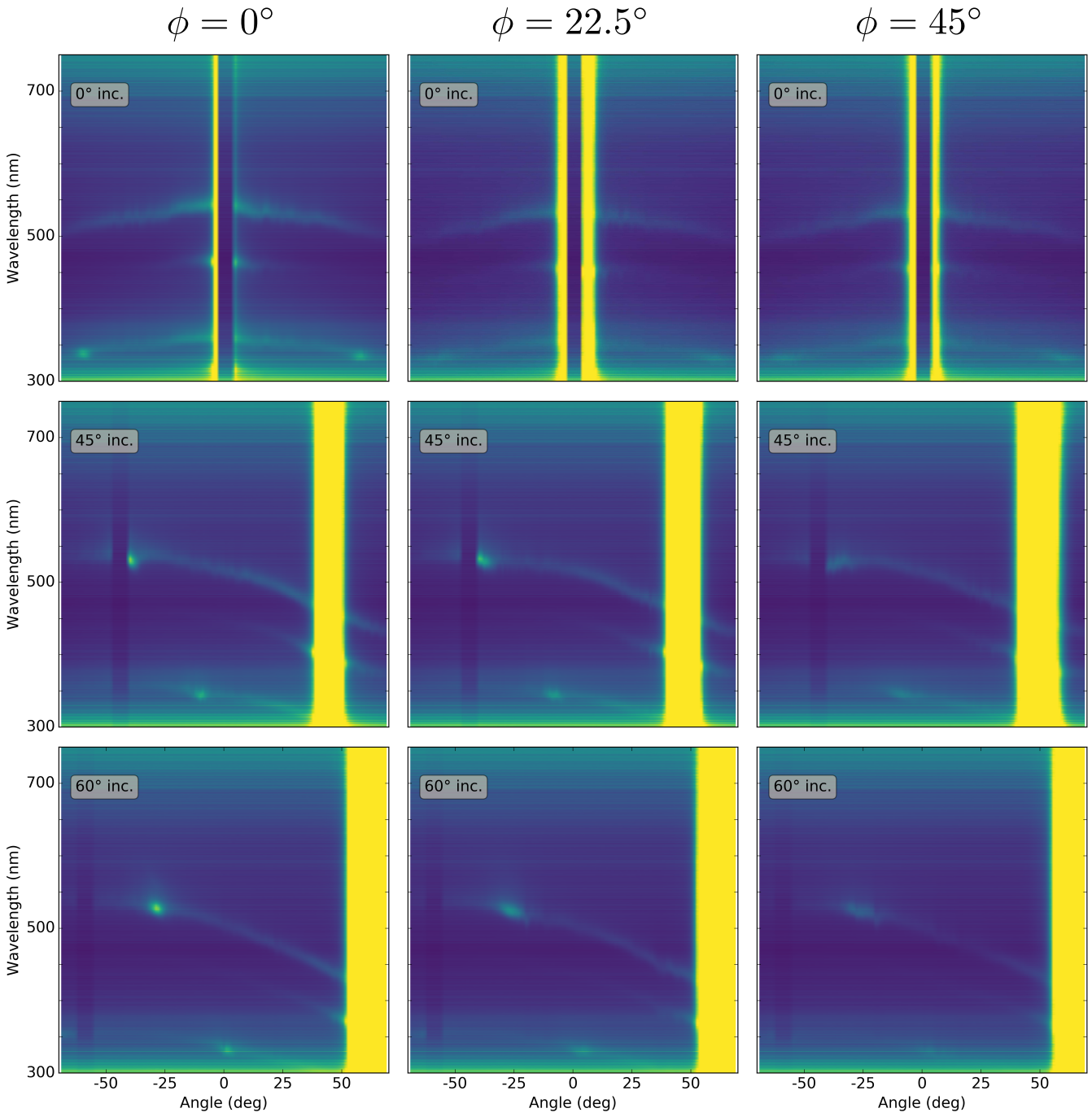

Fig. S4. Measurement of in-plane sample rotation for IR1 wild type. The bacteria were measured at three different incident angles for three different φ rotations (see Fig. 3D) in order to confirm independence of the orientation of the sample. The data are concluded to be similar with a decrease in reflection most likely caused by heating of the sample from the light source.

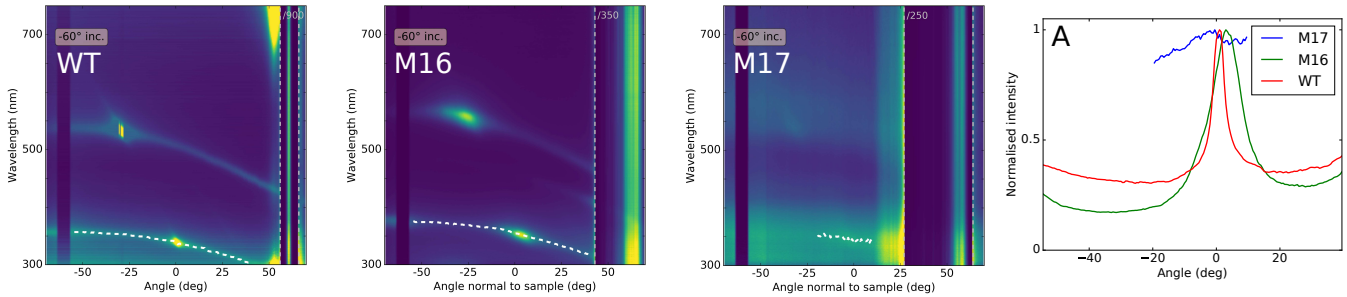

Fig. S5. Peak extraction. WT, M16, M17) The data presented in Fig. 2 with a dashed line indicating from where the peak intensities have been taken from. A) Normalised plots of peak intensities with respect to angle.

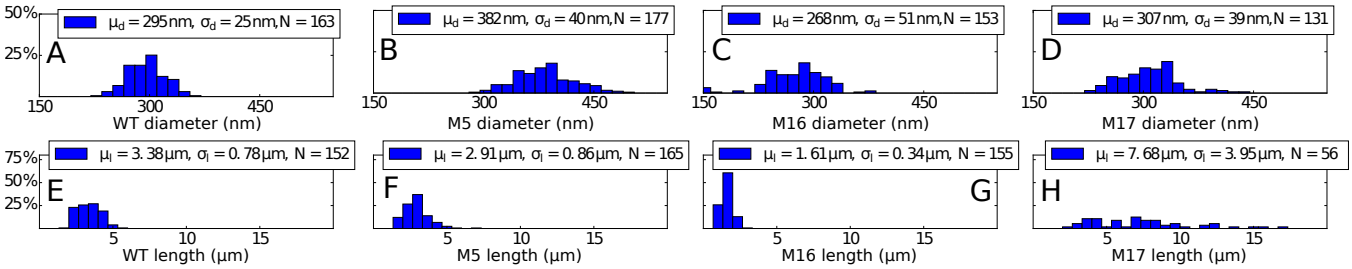

Fig. S6. Bacterium dimensions of WT, M5, M16 and M17. A-H) Bacterium diameters and lengths as measured from several SEM images, with mean (μ), standard deviation (σ) and sample sizes (N) shown. The bins sum to 100%.

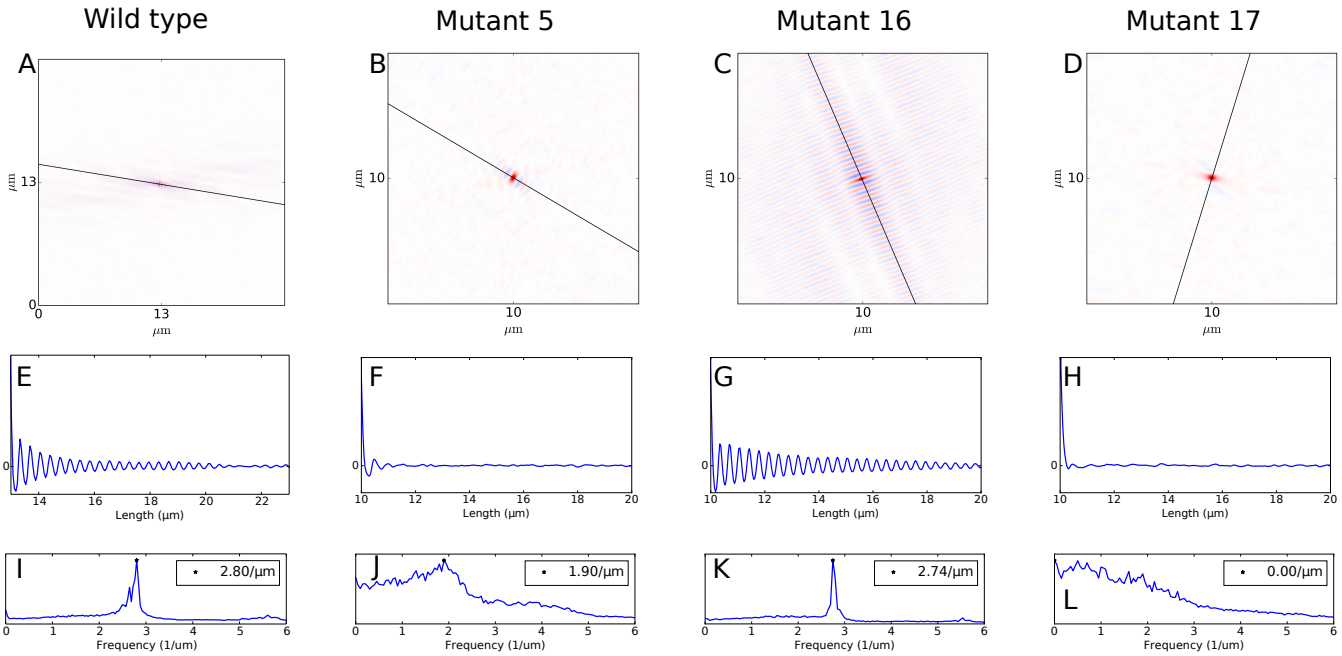

Fig. S7. Autocorrelation analysis on large SEMs in Fig. 2. A-D) Image plots of the autocorrelations with red/blue being positive/negative, respectively, and white equals zero. E-H) Data extracted along the black lines indicated in A-D, where the correlation function is most prominent. I-L) Fourier transforms of the extracted line data from E-H. Peak values show the governing frequency of the periodic repetitions of the cells. The corresponding periods are $357\ \mathrm{nm}, 526\ \mathrm{nm}, 365\ \mathrm{nm}, -$ respectively.

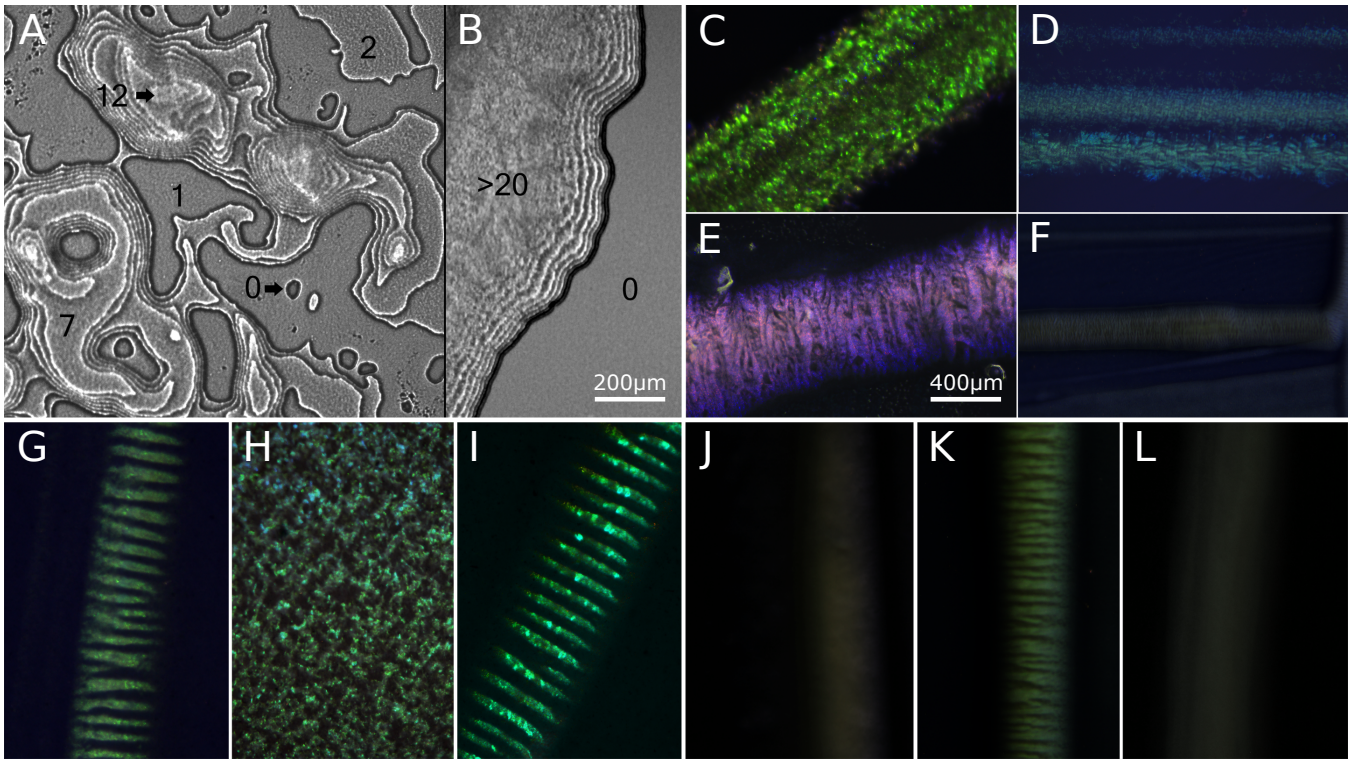

Fig. S8. Motility and iridescence in the *Flavobacteria* IR1 and F52. A-B) Light microscopy of motile and non-motile colony edges. Both images are taken by reflected light microscopy near the edge of a growing colony. A) WT IR1 showing a 'contour map' with each tier being a monolayer of motile cells. B) Mutant 17 with a sharper colony edge and no moving cells. In both images, the numbers refer to the height of that region in cell layers with 0 indicating the agar surface. C) Strain F52 cultured on ASWB agarose. D) F52 with a KO of *gld*J cultured on ASWB agarose. E) WT strain of F52 $1\ \mathrm{h}$ after plating on ASWBC agarose with $50\ \mu\mathrm{g/ml}$ rifampicin. F) F52 with a KO of *gld*J cultured on ASWB with rifampicin and imaged after $1\ \mathrm{h}$. G-L) Culture of WT (G-I) and M17 (J-L) strains of IR1 on ASWBVLow plates, in all cases initiated by a culture streaked from iridescent cells on an ASWBC plate, with iridescence imaged by light microscopy. Panels G,J show iridescence after $30\ \mathrm{min}$ at $22\ ^{\circ}\mathrm{C}$; H,K show iridescence after $16\ \mathrm{h}$; and I,L after $1\ \mathrm{h}$ with $50\ \mu\mathrm{g/ml}$ rifampicin. In panel H rapid outwards migration from the original streak has occurred, obscuring the inoculation. Scale bar is equal for A-B and C-L.

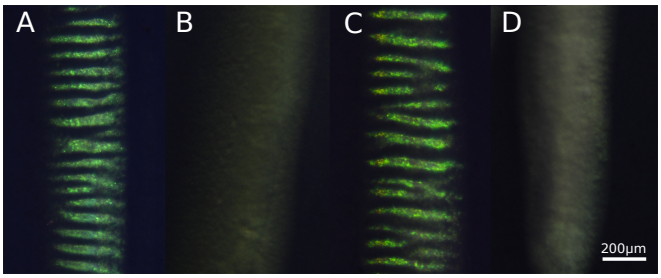

Fig. S9. The effect of metabolic inhibitors on the formation of patterned structural colour on ASWBC agar 30 min after streaking from a plate of IR1 displaying structural colour. A) Control. B) With the addition to the plate of the uncoupler $10\ \mu\mathrm{m}$ CCCP (Carbonyl cyanide m-chlorophenyl hydrazine).C) With $50\ \mu\mathrm{g/ml}$ Erythromycin to inhibit protein synthesis. D) With the addition of $1\ \mathrm{mm}$ sodium azide. In all cases the additives were sufficient to completely inhibit growth. Same scale bar for all panels.

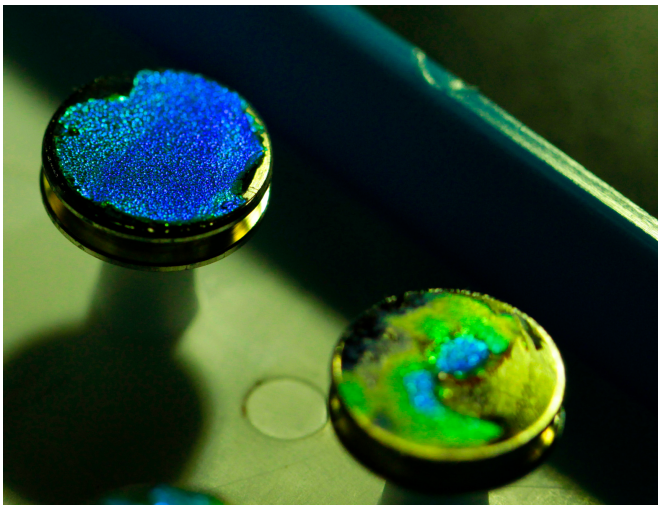

Fig. S10. Examples of dead, dehydrated colonies of IR1 mounted on SEM stubs after critical point drying. Upper stub is a blue shifted mutant S2 and lower stub is the wild type. The stubs are $1\ \mathrm{cm}$ in diameter.

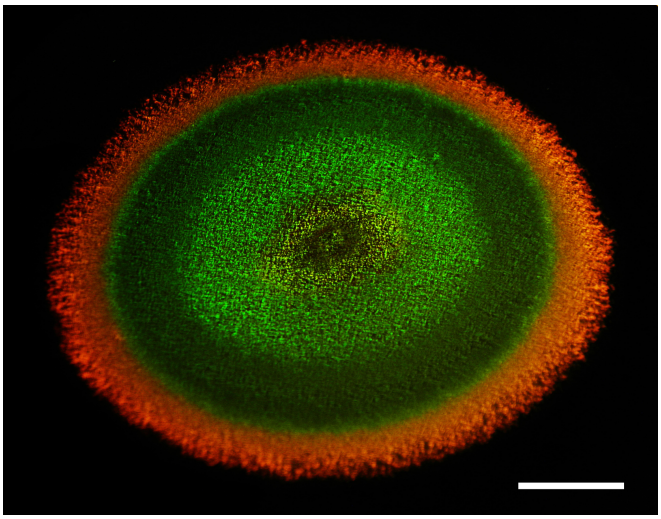

Fig. S11. Example of WT colony cultured on ASWBC agar showing patterning of structural colour. Scale bar indicates $0.4\ \mathrm{mm}$.